

# THE EFFECT OF BAND ENGINEERING OF SEMICONDUCTORS AND OTHER FACTORS ON PHOTOCATALYTIC DEGRADATION OF ORGANIC POLLUTANTS, TOWARDS A SCALE OF PHOTOCATALYTIC EFFECTIVENESS: A MULTIFACTORIAL EQUATION FOR THE PHOTOCATALYTIC EFFICENCE. A REVIEW

MARÍA LUISA VALENZUELA <sup>1\*</sup>, CARLOS DIAZ <sup>2,\*</sup>, AND MARJORIE SEGOVIA <sup>3</sup>

<sup>1</sup>Instituto de Ciencias Aplicadas, Facultad de Ingeniería, Universidad Autónoma de Chile, Av. El Llano Subercaseaux 2801, Santiago, Chile

<sup>2</sup>Departamento de Química, Facultad de Ciencias, Universidad de Chile, Las Palmeras 3425, Ñuñoa, Casilla 653, 7750000, Santiago, Chile.

<sup>3</sup>Aintech, Los Hilanderos 8521, La reina, Santiago, Chile.

## ABSTRACT

The direct conversion of solar energy using a photocatalyst in a degradation of a pollutant reaction is a source of a sustainable and clean environment remediation. In general, photocatalyst are semiconductors that possess valence and conduction bands. These energy bands permit the absorption of photon energy to excite electrons in the outer orbitals of the photocatalyst. Photoexcited electron and hole pairs can subsequently induce a reaction that degrade organic pollutant molecules. Photocatalyst degradation of pollutants is affected by the band level and crystallinity of the photocatalyst among others, therefore, band engineering using chemical modifications as particle size, morphology and physical as band gap could create photocatalyst suitable for the large-scale photodegradation of organic pollutant. In this Review, different factors of the photocatalyst obtained by solid-state, such as size, morphology, band gap and others are analyzed in the photocatalyst efficiency of the degradation of organic contaminant. This review involves binary metal oxide photocatalyst of the MxOy type, prepared from a solid-state route. The photocatalytic degradation of blue methylene using our the solid-state TiO<sub>2</sub>, Fe<sub>2</sub>O<sub>3</sub>, NiO, ReO<sub>3</sub>, IrO<sub>2</sub>, Rh<sub>2</sub>O<sub>3</sub>, Rh/RhO<sub>2</sub>, and the actinide ThO<sub>2</sub> prepared nanostructured metal oxides by a solid state method is described and discussed. Also, other studies of photocatalysis also prepared in solid state for the degradation of methylene blue and reported in the literature are shown and analyzed. With regard the photocatalytic efficiency, factors such as the particle size and morphology, the crystalline phase and the pyrolysis temperature used in the solid-state preparation method are very important. A multifactorial equation that summarizes the main factors that govern the photocatalytic efficiency of a photocatalyst is proposed. A parameterization of these factors is discussed through an equation of the photocatalytic efficiency as a function of these parameters. The importance of each of these parameters/factors in the photocatalytic efficiency against methylene blue degradation is discussed..

**Keywords:** Semiconductors, photocatalytic, organic pollutants.

## INTRODUCTION

Photocatalytic degradation has been proved as a promising method for treatment of wastewater, contaminated with organic and inorganic pollutants. The process, as a means of removal of persistent water contaminants such as dyes and pesticides has attracted the attention of many researchers in recent years [1-3] In recent years, synthetic organic dyes have become one of the leading pollutants in wastewater because of their extensive use in various industries such as plastic, rubber, cosmetics, textile, printing and paper industries as colouring agents [1]. The release of these coloured waste water in the ecosystem cause various environmental issues such as, biochemical oxygen demand (BOD), chemical oxygen demand (COD), increase of toxicity and colour of the water. As a result, the removal of organic pollutants like Methylene Blue (MB), Congo red (CR) and Rhodamine B has been the subject of various researches using different techniques such as chemical oxidation, reverse osmosis, electrochemical process or photochemical degradation, adsorption[2, 3]. Among them, photodegradation and adsorption are the two main reliable and effective methods for the removal of the toxic dyes. Recently, adsorption process has been proved to be an excellent method, which offers significant advantages like easy operations, low cost and reusability of the adsorbent. But this technique transfers pollutants merely from aqueous to solid phase rather than their degradation and generates secondary waste problems. Compared with adsorption, Photocatalysis technology is considered as one of the most promising method for the removal of the carcinogenic organic pollutants because of mineralization of dyes based on solar energy [4].

Among them, photodegradation and adsorption are the two main reliable and effective methods for the removal of the toxic dyes. Recently, adsorption process has been proved an excellent method, which offers significant advantages like easy operations, low cost and reusability of the adsorbent. However, this technique transfers pollutants merely from aqueous to solid phase rather than their degradation and generates secondary waste problems. Compared with adsorption, Photocatalysis technology is considered as one of the most promising method for the removal of

Recently, the application of metal oxide semiconductors in the advanced oxidation process (AOP) has gained wide interest for the treatment of dye wastewater owing to its good degradation efficiency, low toxicity and physical and chemical properties [5,6].

Usually photocatalyst are prepared by solution methods but solid-state methods have some advantages [7] Thus, solvent-less synthesis of nanostructures is highly significant due to its economical, eco-friendly and industrially viable nature. In solution methods, the nanoparticles must be separated and isolated as a solid, which is done with methodologies that produce alterations such as agglomeration, which ultimately produces a loss of the characteristic properties of nanodimensionality. On the contrary, in the solid-state, the photocatalyst is formed in the solid state, being ready to be used [6].

The general mechanism of action of a heterogeneous photocatalyst is well-established [7]. When ultraviolet (UV) radiation from sunlight or an illuminated light source (fluorescence lamp) is shone on the semiconductor, an electron in the valence band will receive energy and become excited see Fig 1. If the radiation energy supplied to the semiconductor is higher than the energy difference between the valence and conduction bands (band gap), the electron can be promoted into the conduction band, creating a negative electron in the conduction band ( $e^-_{cb}$ ) and a positive hole in the valence band ( $h^+_{vb}$ ), (Equation (1)). This is referred to as the photoexcited state of the semiconductor. Depending on the  $E_g$  value, of the photocatalyst, the irradiation used will be in the Uv range or in the Visible range, see figure 2.

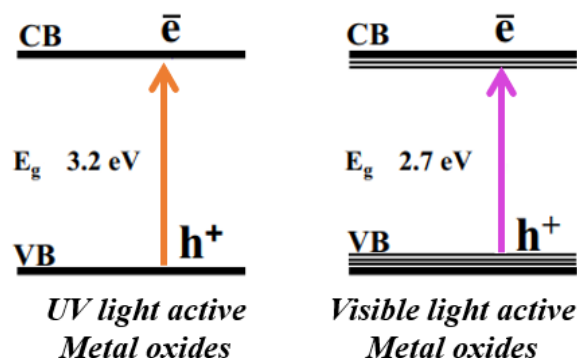
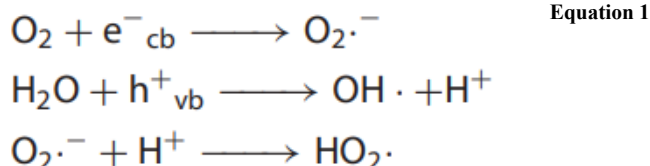


**Figure 1:** Band gap and UV light active metal oxides and visible light active metal oxides showing photoexcitation. Adapted from reference 8. -

The conduction band electron and valence band hole are able to migrate to the surface of the semiconductor generating a redox environment for the photocatalytic degradation of the dye molecule. Oxygen present in the wastewater, will scavenge the conduction band electron ( $e^-_{cb}$ ) forming a superoxide oxygen radical ( $O_2^{\cdot-}$ ), (Equation (1)). The radical  $O_2^{\cdot-}$  will then react with a proton to form a hydroperoxide radical ( $HO_2^{\cdot}$ ), (Equation (3)). On the other hand the holes  $h^+$  generates in the valence band, by effect of the UV or visible light on the semiconductor, see figure 1, to react with  $H_2O$ , see equation 2, to give  $OH^{\cdot}$  radicals.

These  $O_2^{\cdot-}$ ,  $OH^{\cdot}$  and  $HO_2^{\cdot}$  radicals will repeatedly attack the dye molecule and effectively degrade it to less harmful, simple molecules, such as  $CO_2$ ,  $H_2O$  and  $N_2$ .



For photocatalyst obtained by a solution method, the photocatalytic efficiency strongly depends on the size of the nanocrystals and the surface area measured by their morphology. In addition, the band gap of the photocatalyst can be important in some cases. [9] For photocatalyst obtained by a solid-state method, little is known about the parameters involved in the photocatalytic efficiency; however, preliminary studies suggest that morphology (porous) and pyrolysis temperature are important factors [10]. These factors in some cases may be more important than the band gap of the photocatalyst.

#### Organic Dyes pollutants

The production of synthetic dyes is on the increase due to their high demand, most especially in the textile and clothing industries. A few examples of synthetic dyes are aniline blue, alcian blue, basic fuchsin, methylene blue, crystal violet, toluidine blue, and congo red. Methylene blue (3,7-bis(dimethylamino)phenothiazine chloride tetra methylthionine chloride) is one of the synthetic dyes that is applied in large amount as colorant for papers, in wool, silk, and cotton [10-18].

Treatment of wastewater containing MB dye before discharging into the environment, is of great importance due to its harmful impacts on water quality and perception [17]. Various methods are reported to remove MB and other textile dyes from industrial wastewater. These include adsorption/biosorption phytoremediation coagulation electrocoagulation [vacuum membrane distillation, liquid-liquid extraction, ultrafiltration, nanofiltration, microwave treatment, biodegradation, hybrid systems [19] etc.

Hence, there is a need to develop an environmentally friendly, efficient technology for removing MB from wastewater. Photodegradation is an advanced oxidation process widely used for MB removal. It has the advantages of complete mineralization of dye into simple and nontoxic species with the potential to decrease the processing cost.

MB is a representative organic dye and stable under visible light irradiation [19]. Due to its stability, it cannot be degraded efficiently just by photolysis or catalysis alone. It was reported that 7.9% of MB dye was removed through photolysis after 10 h irradiation time, and only 10% degradation of MB occurred after 24 h in the presence of a catalyst without light irradiation [19]. It was also observed that no/negligible decomposition occurred without a catalyst under visible light. Similarly, no degradation was observed in the acidic and neutral medium in the dark and under sunlight irradiation without using a catalyst. In the basic medium, photolysis occurs rapidly because of the formation of the hydroxyl ions, which is a key radical for dye degradation. However, raising the temperature has a negligible effect and under argon, atmosphere degradation completely stopped [19]. In figure 2 a schematic representation of the degradation mechanism is presented.

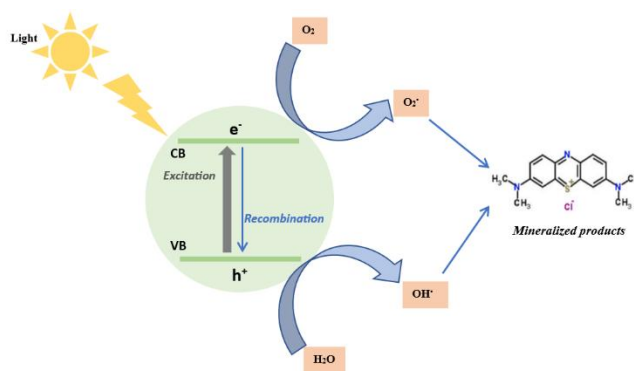


**Figure 2:** General scheme of the degradation mechanism of methylene blue by photocatalyst –Adapted from reference 19.

Photodegradation of MB is an efficient approach because MB can also function as a photocatalyst sensitizer.

Semiconductor metal oxides have proven to be efficient photocatalysts in the degradation of met ability and reusability [10-12]. The significant features of the photocatalytic system are the desired band gap, suitable morphology, high surface area, stability and reusability.

Metal oxides such as oxides of vanadium, chromium, titanium, zinc, tin, cerium and others having these characteristics follow similar primary photocatalytic processes such as light absorption, which induces a charge separation process with the formation of positive holes that are able to oxidize organic substrates [10-12]. In this process, a metal oxide is activated with either UV light, visible light see figure 2, or a combination of both, and photoexcited electrons are promoted from the valence band to the conduction band, forming an electron/hole pair ( $e^-/h^+$ ) see figure 2. The photogenerated pair ( $e^-/h^+$ ) is able to reduce and/or oxidize a compound adsorbed on the photocatalyst surface. The photocatalytic activity of metal oxide comes from two sources: (i) generation of  $\cdot OH$  radicals by reaction of  $H_2O$  with holes  $h^+$  equation 2, (ii) generation of  $O_2^{\cdot-}$  by reaction of  $O_2$  with  $e^-$  equation 1. Both the radicals and anions can react with pollutants to degrade or otherwise transform them to lesser harmful byproducts [5,6]. There are many catalysts reported in the literature for this exciting process. Among these metal oxides,  $TiO_2$ ,  $ZnO$ ,  $SnO_2$  and  $CeO_2$ , which are abundant in nature, have also been extensively used as photocatalysts, particularly as heterogeneous photocatalyst since several decades [7,10]. However, some lesser-known semiconductor metal oxides such as  $ReO_3$ ,  $IrO_2$ ,  $Rh_2O_3$ ,  $Rh/RhO_2$ , and the actinide  $ThO_2$  have also been tested as methylene blue photocatalysts, finding significant photocatalytic activity [20-25].

#### Factors affecting the efficiency of a metal oxide type photocatalyst

For metal oxides semiconductors prepared in solution several factors affect the photocatalytic efficiency for degradation of methylene blue. The physicochemical properties of the metal oxides are crucial for the virtuous photocatalytic performance, which are typically size, shape, morphology, and composition dependent [7,9,10,26,27]. The synthetic procedure employed can control the size, shape and morphology of the materials prepared, which can contribute towards the development of certain properties of the photoactive materials. This can facilitate the formation of powders or thin films with the required characteristics that improve the performance of the catalyst [6,7,10,26,27]. In this context, the methods for preparing solid state nanostructured semiconductor metal oxides have advantages since they are obtained in a single step as solid powders and no treatment is required to obtain them in this form, using a solution method, which their isolation to solid-state, involves procedures that normally produce agglomeration with loss of nanometric properties. It is also the source and type of the light used that can affect the performance of the material as a photocatalyst [8-10]. Thus, photocatalysts that have a band gap above 3.2 eV need UV irradiation, while those that have a band gap below 2.7 eV need Visible radiation see figure 2. Hence, in conclusion, knowledge of the different synthetic procedures employed for the preparation of photocatalytic materials in solid-state should be considered necessary and they are a constant challenge. The search for new photocatalyst having desired characteristics to induce the oxidation of organic substrates or

pollutants under visible light irradiation is encouraging. The metal oxides should be ecologically affable and preparation via inexpensive routes should be the main attention. These are the major concerns from the synthetic and industrial points of view, which should be the primary focus of the researchers involved.

#### Factors that govern the photocatalytic efficiency of photocatalyst obtained in the solid state

Although, as mentioned above, the factors that are involved in the photocatalytic efficiency of photocatalyst obtained by a solution method are well known, for photocatalyst obtained in the solid state, little is known about the factors that govern their photocatalytic efficiency. In this section we will discuss what is known about the photocatalytic efficiency of photocatalysts obtained in the solid state and its possible factors that modulate it.

The examples discussed below involve two cases for the obtention procedures for solid-state :

1. The synthesis method involves several steps, all in solid state
2. The synthesis method involves some previous steps in solution, but the last step is a solid state process

#### Factors that influence the photocatalytic efficiency in the solid state

Previously we have proposed a general equation 2, which would account for the factors involved in the catalytic efficiency, PE, of a photocatalyst prepared in the solid state:

$$PE = a \text{ band gap} + b \text{ particle morphology} + c \text{ particle size} + d \text{ crystalline phase} + e \text{ pyrolysis temperature.} \quad \text{Equation 2}$$

where the factors band gap, particle morphology, particle size crystalline phase and pyrolysis temperature refer to the properties and preparation conditions of the photocatalyst [10].

Examining some preliminary results of the catalytic efficiency of photocatalyst obtained by a solid-state method against methylene blue it seems that in general morphology is one of the most important factors in photocatalytic efficiency. This is especially true when the other factors such as band gap and particle size as well as crystalline phase and pyrolysis temperature where appropriate are basally favorable factors. Next, the results in the literature on the degradation of methylene blue using photocatalyst prepared in the solid state will be analyzed in relation to the effects of morphology, particle size, band gap and crystalline phase when appropriate. Additionally, other less recurring effects such as the nature of the metal precursor used and the preparation method used to obtain the photocatalyst, factors not explicitly considered in the equation 2, can sometimes also be important in the efficiency of the photocatalyst.

#### TiO<sub>2</sub>

The titania to be used as photocatalyst was obtained by pyrolysis of the (Cp<sub>2</sub>TiCl<sub>2</sub>)(Quitosano) (I), (Cp<sub>2</sub>TiCl<sub>2</sub>)(PS-co-4-PVP) (II), (TiOSO<sub>4</sub>)(Chitosan) (III), (TiOSO<sub>4</sub>)(PS-co-4-PVP) (IV), (TiO(acac)<sub>2</sub>)(Chitosan) (V), and (TiO(acac)<sub>2</sub>)(PS-co-4-PVP) (VI) macromolecular precursors under air and at several temperatures (500 °C, 600 °C, 700 °C, and 800°C [10,20]. In this case, Band gaps, morphology, crystalline phase, and photocatalytic efficiency depend on the nature of the Ti precursor and the pyrolysis temperature. Thus, the higher efficiency photocatalytic efficiency against the degradation of methylene blue is given for the precursor Chitosan(TiOSO<sub>4</sub>)<sub>n</sub> pyrolyzed at 800 °C [10, 20]. This was of 87% degradation after 25 min. Under these conditions, the anatase phase obtained presents a morphology of highly porous fibers and to a lesser extent the particle size, 6.9 nm which explains the high PE since all other factors were similar for the other TiO<sub>2</sub> nanoparticles obtained at other temperatures.

#### CeO<sub>2</sub>

In this case CeO<sub>2</sub> NPs were synthesised from the precursors, cerium nitrate hexahydrate (Ce(NO<sub>3</sub>)<sub>3</sub>·6H<sub>2</sub>O) and NaOH in a 1:2 ratio. excess NaOH, the precipitate was filter using whatmann filter paper and washed with distilled water and ethanol [28]. After some solution procedure precipitate was dried for 1 hr at 100°C and then calcined for 2 hr at 1000–1100°C to get a fine pinkish powder of CeO<sub>2</sub>. The as prepared semiconductor oxide has a band gap of 3.28 eV determined from its diffuse reflectance spectrum. Then using a UV light source

a photodegradation efficiency was 90.84% in 90 min. The high photocatalytic capacity of the CeO<sub>2</sub> catalyst can be attributed to the porosity exhibited by this semiconductor. The effect of other parameters such as particle size, temperature pirlisis and band gap, on the photodegradation efficiency were not investigated.

On the other hand, in another study CeO<sub>2</sub> is prepared by a solid state method through the pyrolysis of Ce(OH)<sub>4</sub> prepared from (NH<sub>4</sub>)<sub>2</sub>Ce(NO<sub>3</sub>)<sub>6</sub> and ammonia [29]. The size of the CeO<sub>2</sub> particles calcined at 200, 400, 600, and 900 °C were 3.2, 4.0, 8.8, and 26.6 nm, respectively, calculated using the Scherrer approximation. Degradation of the MB molecules occurred under UV-Vis irradiation. The effect of calcination temperature, pH and natural anions in the photocatalytic efficiency of the degradation of methylene blue, was investigated. The results are shown in tables 1, 2 and 3. From table 1 it can be seen that the % degradation has a maximum at 600 °C with a particle size of 8.8 nm and the minimum at a temperature of 200 °C with a particle size of 3.2 nm. As has been observed in other studies, the maximum degradation is obtained at an intermediate value of particle size values between the smallest and the largest. At 600 it may be that a crystalline phase is formed that is more porous with a greater surface area. Photocatalytic activity is affected by particle size, crystallinity, and surface properties. These factors are controlled by changes in the preparation method, the co-catalyst loading and foreign elements.

**Table 1. Degradation efficiency of MB (20 mg/L) at pH 7 catalyzed by CeO<sub>2</sub> nanoparticles (0.5 g/L) calcined at different temperatures.** (Adapted from reference 29).

Calcined at different temperatures	% Degradation
200°C	31
400°C	36
600°C	43
900°C	38
Without CeO <sub>2</sub>	20

**Table 2. Degradation efficiency of MB (20 mg/L) catalyzed by CeO<sub>2</sub> nanoparticles (1.0 g/L) at different pH values.** Adapted from reference 29.

Different pH values	% Degradation
2	25
4	45
7	85
9	78
11	62
12	65

**Table 3. Effect of negative ions on the degradation efficiency of MB within 125 min.** Adapted from reference 29.

Negative ions	% Degradation
Chloride	62
Bicarbonate	72
Sulfate	78
Nitrate	85
Persulfate	95
Chlorate	92
Bromate	91
Iodate	90

On the other hand, the pH study on photocatalytic efficiency, see table 2, showed that the optimal pH is 7, for which a photocatalytic efficiency of 85% was obtained. Also an study of the effect of the presence of various anions in the study solution, Figure 3, showed that the anion that most favors the efficiency of photodegradation is S<sub>2</sub>O<sub>8</sub><sup>2-</sup>.

#### ZnO

ZnO is a semiconductor with a ban gap of 3.21 e V. Therefore, its photocatalytic activity, according to the scheme shown in figure 1, requires irradiation in the visible range. Few examples of photocatalysis using nanostructured ZnO obtained from a solid-state method have been reported. Saravana [30] obtained ZnO by pyrolysis Zn<sub>4</sub>O(CH<sub>3</sub>COO)<sub>6</sub>. The photocatalyses were performed using UV source. The photocatalytic efficiency against the degradation of methylene blue was 85%. In addition, a study was made of the effect of the sample treatment, using the same precursor but using other methods

such as the precipitation and sol-gel method, finding that the photocatalytic efficiency depends on this factor. The efficiency of the MB degradation using the 3 different preparation methods are: sol-gel 99 %, precipitation 98 % and thermal decomposition 85 %. Since the band gap value does not seem to influence the photocatalytic efficiency, 3.48, 3.31 and 3.27 respectively, if the ZnO particle size seems to be important, 16, 22 and 30 nm respectively being the smallest value of particle size for ZnO obtained from sol-gel the cause of the highest value.

Also, the larger surface area could contribute to this higher photocatalytic efficiency: 10.5, 9.4 y 8.2 respectively. Photocatalytic efficiency measurements were not carried out, varying other parameters.

## CuO

Setyaningtyas prepare CuO nanostructured from thermal treatment of  $\text{Cu}(\text{OH})_2$  previously prepared by a hydrothermal method [31]. A study of the effect of pH on the efficiency in the degradation of methylene blue results in a maximum of 64.97% at pH 9 under visible light irradiation, with the optimum irradiation time of 120 minutes. The photodegradation mechanism occurs due to the presence of hydroxyl radicals and holes. The reaction rate follows second order kinetics. The effect of other parameters such as particle size, morphology on the photodegradation efficiency were not investigated

In another study Bharali prepare CuO nanoparticles through a heat treatment of the precursor  $\text{Cu}_2\text{Cl}(\text{OH})_3$  in air atmosphere at 400 °C [32]. The average size of the nanostructured CuO was found to be 4.36 nm. The porous CuO was employed for oxidative degradation of different dye molecules in the presence of  $\text{H}_2\text{O}_2$ . The photocatalyses were performed using a Visible source. The as synthesized CuO nanostructure exhibits high catalytic activity for the degradation of methylene blue of 100% after 40 min at 65 °C. The high photocatalytic efficiency was attributed to the highly porous morphology as determined by SEM.

Adhyapak et al [33]. prepare CuO from thermal treatment of the precursor  $\text{CuSO}_4 \cdot 5\text{H}_2\text{O}$  (PVP). The as prepared cupric oxide having a spherical shape with a particle size exhibit a mean diameter of 62.2 nm. In addition, CuO prepared using the same Cu precursor but modifying the stabilizer and the reducer has different photocatalytic capacity. The photocatalysis was carried out using sunlight. Table 4 gives the values of the parameters, nanocrystal size, band gap, and % degradation. The CuO that produces the greatest photodegradation of methylene blue is sample 4 symbolized HT2, which is the one with the smallest size and the highest band gap value with a platelet-like morphology. Unlike other semiconductors of the metal oxide type in which the band gap value It's not that important a factor in this case it is. On the other hand, in accordance with other semiconductors of the metallic oxide type, in which morphology is a preponderant factor, in this case morphology is also important, the platelet like morphologies res being the most effective. In relation to the particle size, in some cases, but not in all, it is an important factor, being in this case the smallest size value that produces a greater photocatalytic efficiency see table 4. It seems that the factors involved in the efficiency of photocatalysts in the degradation of methylene blue depend on specific factors of the nature of each semiconductor of the metal oxide type. This factor, not yet known, would be associated with the properties of each photocatalyst.

**Table 4** Size particle, Band Gap and Degradation efficiency of CuO prepared by several methods

Method <sup>1</sup>	Size (nm)	Band Gap	% Degradation	
1	CP <sub>1</sub>	53.63	2.17	72.57
2	CP <sub>2</sub>	77.03	2.43	93.48
3	HT <sub>1</sub>	41.56	2.36	49.71
4	HT <sub>2</sub>	36.01	2.58	95.71

<sup>1</sup> CP<sub>1</sub>, CP<sub>2</sub>, HT<sub>1</sub> and HT<sub>2</sub> Different preparation methods starting from  $\text{CuSO}_4 \cdot 5\text{H}_2\text{O}$  see [33]

## NiO

NiO is a p-type semiconductor with  $E_G = 3.5$  eV with multiple practical applications. Several examples of NiO preparation have appeared and some have been tested as methylene blue. Photocatalysis. Shrivastava et al [34] prepare

nanostructured NiO by a easy straightforward chemical route by utilizing  $\text{NiCl}_2$  and  $\text{NaHCO}_3$  as a precursor followed by calcination at 450°C for 2 h. The as prepared nanostructured NiO has average crystalline Size 6.36 nm. The extent of photocatalytic degradation of MB using UV source was found to be 98.7 % at pH 2. The kinetic investigation of photocatalytic degradation followed a pseudo-first-order rate kinetics for MB dye with rate constant  $4.6 \times 10^{-1}$ . The effect of other parameters such as particle size, morphology on the photodegradation efficiency were not investigated.

In another approximation Diaz et al. [35], prepares nanostructured NiO through pyrolysis of the macromolecular complexes Chitosan• $(\text{NiCl}_2 \cdot 6\text{H}_2\text{O})_x$  and PS-co-4-PVP• $(\text{NiCl}_2 \cdot 6\text{H}_2\text{O})_x$ . The NiO nanoparticles with particle sizes close to 50 nm and band gap values of 4.15 eV and 4.16 eV, exhibit a photocatalytic activity of 71 % and 68 % respectively using UV source irradiation. No studies of photocatalytic activity as a function of size or other parameters were made.

## Fe<sub>2</sub>O<sub>3</sub>

Diaz et al. prepared  $\text{Fe}_2\text{O}_3$  by pyrolysis of the Chitosan $(\text{FeCl}_2)_y$ , Chitosan $(\text{FeCl}_3)_y$ , PS-b-4-PVP $(\text{FeCl}_2)_y$ , and PS-b-4-PVP $(\text{FeCl}_3)_y$  macromolecular complexes under air and at 800 °C [42]. The product was  $\text{Fe}_2\text{O}_3$  in the hematite phase in all the cases. The bandgap of the as-prepared  $\text{Fe}_2\text{O}_3$  ranged from 1.83 eV to 2.12 eV, which indicated an effective photocatalyst behavior, under UV-visible irradiation [36]. The highest photodegradation was observed for  $\text{Fe}_2\text{O}_3$  obtained by a solid state method, from the precursor  $\text{FeCl}_2 \cdot (\text{Chitosan})$  which produce 73.4% and 94.6 % of degradation at 60 min and 150 min respectively. Again, the factor b particle morphology through porous materials appears to be the origin of the high photocatalyst efficiency found. Comparison with  $\text{Fe}_2\text{O}_3$  obtained by another preparation solution methods [36], indicate that the here described solid-state preparation method for  $\text{Fe}_2\text{O}_3$  is a comparable efficient photocatalyst for degradation of methylene blue. The porous morphology normally obtained by the solid-state preparation method can be they may be the cause.

In another approach,  $\text{Fe}_2\text{O}_3$  was obtained by calcination of a solid mixture of ferric nitrate and malic acid at 600°C [37]. The average crystalline size of 34.55 nm was calculated for the as-prepared  $\alpha\text{-Fe}_2\text{O}_3$  nanoparticles with a band gap energy (Eg), of 2.13 eV. Then the appropriate irradiation was visible light. After 70 min of exposure to visible light, 97% degradation of MB was observed. No other effects such as precursor pyrolysis temperature or  $\text{Fe}_2\text{O}_3$  nanoparticle size on methylene blue degradation efficiency were investigated.

Saber Lassoued, prepare  $\text{Fe}_2\text{O}_3$  by thermal treatment of  $\text{Fe}(\text{OH})_3$  at 700 °C [38]. The as prepared iron oxide nanoparticles having a particle size of 22 nm and a band gap of 2.14 eV showed a photoluminescence of 89 % toward degradation of methylene blue in 140 min. Other effects such as morphology, pyrolysis temperature and particle size on the photodegradation efficiency of the dye were not studied.

Finally, Liu et al [39] prepare  $\text{Fe}_2\text{O}_3$  from a solid mixture of  $\text{FeCl}_3 \cdot 6\text{H}_2\text{O}$  with sodium dodecyl sulfate and calcined at various temperatures. The as prepared  $\text{Fe}_2\text{O}_3$  exhibits particle sizes and band gap values depending on the calcination temperature. The as prepared iron oxide nanoparticles at 500 °C has a particles size and a band gap of 1.65 eV. The photocatalytic degradation tests indicate that the highest efficiency in the degradation of methylene blue was obtained for the sample of the precursor pyrolyzed at 500 C with a 73.2% degradation in 180 min. In the presence of  $\text{H}_2\text{O}_2$  the efficiency in the degradation of MB increases to 90% in just 40 min. No other parameters on the photocatalytic degradation were studied.

## SnO<sub>2</sub>

Luque Morales prepare  $\text{SnO}_2$  nanoparticles from heat treatment at 400 °C for 1 h of a basic salt of Sn [40]. The nanoparticle sizes for the NPs thus prepared were in the range 16nm-22 nm while their band gap was found to be approximately 3.6 eV. The NPs yielded great photocatalytic activity capable of degrading methylene blue (MB) dye under ultraviolet radiation and solar radiation, achieving degradation percentages of 90% and 83% of MB under UV and solar radiation at 90 and 180 min, respectively. The work does not include the effect of other parameters such as particle size, morphology and pH, among others, on the photocatalytic efficiency in the degradation of methylene blue. No other parameters on the photocatalytic degradation were studied.

On the other hand Sadeghzadeh-Attar [41] prepare SnO<sub>2</sub> nanotubes using hexafluorostannate template-based liquid phase deposition as a precursor was applied to fabricate amorphous SnO<sub>2</sub> nanotubes and finally thermal treatment of these to give SnO<sub>2</sub> nanocrystals nanotubes. The dimensions of the nanotubes where the mean crystallite size was calculated to be about 6.5, 9.4 and 15.8 nm for the SnO<sub>2</sub> nanotubes calcined at 500, 600 and 700 °C for 1 h, respectively. The dimensions of the nanotubes where the mean crystallite size (d) was calculated to be about 6.5, 9.4 and 15.8 nm for the SnO<sub>2</sub> nanotubes calcined at 500, 600 and 700 °C for 1 h, respectively. The estimated values of band gap energy for SnO<sub>2</sub> nanotubes were obtained 3.31, 3.36, 3.60, 3.74, 3.87 and 3.90 eV for the samples of as prepared and calcined at 300, 400, 500, 600 and 700°C, respectively. These values indicated a red shift with increasing calcination temperature, which can be attributed to crystallite size, crystallinity and defect associated with oxygen vacancies. The photocatalytic activity of the SnO<sub>2</sub> nanotubes first increased with increasing the calcination temperature up to 600 °C, and then decreased upon calcination at 700 °C. It clearly indicates that the sample calcined at 600 °C exhibited the best photocatalytic activity, 90.7% MB. The dimensions of the nanotubes where the mean crystallite size (d) was calculated to be about 6.5, 9.4 and 15.8 nm for the SnO<sub>2</sub> nanotubes calcined at 500, 600 and 700 °C for 1 h, respectively. The estimated values of band gap energy for SnO<sub>2</sub> nanotubes were obtained 3.31, 3.36, 3.60, 3.74, 3.87 and 3.90 eV for the samples of as-prepared and calcined at 300, 400, 500, 600 and 700°C, respectively. These values indicated a red shift with increasing calcination temperature, which can be attributed to crystallite size, crystallinity and defect associated with oxygen vacancies [41]. The photocatalytic activity of the SnO<sub>2</sub> nanotubes first increased with increasing the calcination temperature up to 600 °C, and then decreased upon calcination at 700 °C. It clearly indicates that the sample calcined at 600 °C exhibited the best photocatalytic activity, degraded 90.7% in 180 min, compared to the other calcination temperatures at 300, 400, 500 and 700 °C, which were 72.4%, 78.4%, 84.5% and 87.2%, respectively. Generally, the improvement of the photodegradation performance can be attributed to several separated factors such as morphology, particle size, porosity, crystallinity, and surface area. High surface area could provide more active sites for photodegradation reactions and promote the efficiency of the electron-hole separation. In this study the focus was on two factors: namely specific surface area and crystallinity. It was found that the surface area of nanotubes decreases continuously with calcination temperature. The growth of the particles leads to the decrease of the surface area and photocatalytic activity of SnO<sub>2</sub> nanotubes. On the other hand, the crystallinity of the SnO<sub>2</sub> nanotubes for this study became higher with calcination temperature. On the other hand it is known that higher crystallinity with increased calcination temperature means fewer defects, which leads to increase in band gap energy and definitely favors the photocatalytic activity. The defects may serve as the recombination centers for photoexcited electron-hole pairs during photodegradation, which would decrease the photocatalytic activity [41]. From these results, it can be concluded that the more photodegradation efficiency of the sample calcined at 600 °C than the ones calcined at other temperatures was mainly caused by combined effects of crystallinity and specific surface area. This can be attributed, among others, to the highly porous nature of nanotubes [41]. Therefore in this study, the calcination temperature of the SnO<sub>2</sub> nanotubes played an important role in the degradation of the MB dye. At this temperature, the nanotubes with the highest porosity are produced, which induces an optimal morphology (equation factor b) to be the most important factor in catalytic efficiency.

In another approximation Choib[ 42] prepare SnO<sub>2</sub> using a solid state method by calcining a basic Sn salt for 2 h at 380 C. The SnO<sub>2</sub> nanoparticles thus prepared have an average size of 4.5 nm The maximum photodegradation of MB achieved in this study was 79% after an irradiation time of 180 min. No other effects such as particle size, calcination temperature or pH on the photocatalytic effectiveness of SnO<sub>2</sub> were investigated.

### Co<sub>3</sub>O<sub>4</sub>

Miottello [43] prepares Co<sub>3</sub>O<sub>4</sub> thin coatings by using four different methods, namely: (1) PLD, (Pulsed laser deposition) (2) EBD, (Electron beam deposition), (3) sol-gel method, and (4) electroless deposition. All these methods involve a last step with heat treatment except the PLD method. Co<sub>3</sub>O<sub>4</sub> is a semiconductor that has a band gap of 1.5 eV. Then by irradiation with light in the Visible range it will produce enough e<sup>-</sup> and h<sup>+</sup> which in turn will produce O<sub>2</sub><sup>-</sup> and OH<sup>•</sup>, see Table 5, to degrade methylene blue. As shown in Table of Table 5, the photocatalytic efficiency is affected by the form of sample preparation, the size

and the band gap of the Co<sub>3</sub>O<sub>4</sub> nanoparticles. In turn, the way the NPs are prepared affects in some way the size and band gap of the nanoparticles. The morphology of the Co<sub>3</sub>O<sub>4</sub> obtained by a PLD method seen by SEM shows more separated spheres than those observed for the cobalt nanoparticles obtained by the other methods, see Figure 3 for which more agglomerated morphologies were observed.

**Table 5** Size particle, Band Gap and Degradation efficiency of Co<sub>3</sub>O<sub>4</sub> prepared by several methods

Methodology	Size (nm)	Eg (eV)	% Degradation
PLD	18	1.55	99
EBD	27	1.51	99
Sol-gel	20	1.43	90
Electroless –Deposition	38	1.53	76
Co <sub>3</sub> O <sub>4</sub> powder by precipitation method	48	---	46

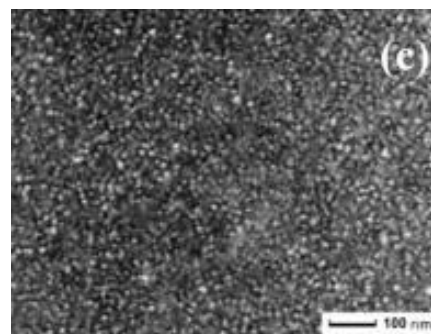


**Figure 3:** SEM image of Co<sub>3</sub>O<sub>4</sub> prepared from a PLD method (Adapted from reference 43).

Farhadi [44] prepare Co<sub>3</sub>O<sub>4</sub> nanorods by thermal microwave-assisted solid state decomposition of the precursor CoC<sub>2</sub>O<sub>4</sub>·2H<sub>2</sub>O. TEM and SEM images showed that the Co<sub>3</sub>O<sub>4</sub> nanorods have a length of 1-3 μm and diameter of 40-80 nm. The optical spectrum indicated two direct band gaps at 2.20 and 3.60 eV with a blue shift compared with the bulk sample. The photocatalytic activity of Co<sub>3</sub>O<sub>4</sub> nanorods was investigated for the degradation of methylene blue (MB) as a model of dye pollutants in the presence of H<sub>2</sub>O<sub>2</sub> as a green oxidant. The dose of photocatalyst used affects the efficiency of the photocatalyst. So when Co<sub>3</sub>O<sub>4</sub> dosages from 10 to 20 and then to 30 mg, the photocatalytic efficiency of MB degradation was found to be 54, 83 and 100% respectively, in 160 min. Other parameters such as particle size and morphology on photocatalytic efficiency are not studied.

### MnO<sub>2</sub>

Few examples of degradation of methylene blue by manganese oxides semiconductors prepared by a solid state method have been reported. (β-MnO<sub>2</sub>) nanorods were prepared by Yang [45] from the precursor MnOOH nanorods by calcination at 350 °C in air in a furnace for 4 h and this gave a black powder. The as-prepared β-MnO<sub>2</sub> nanorods were shown to be phase-pure single crystallites with diameters of 30–400 nm and lengths of tens of micrometers. The catalytic efficiency of the as-prepared one-dimensional β-MnO<sub>2</sub> nanorods as catalysts in the oxidation of methylene blue dye in the presence of H<sub>2</sub>O<sub>2</sub> was 95% in only 15 min. The catalytic performance of the β-MnO<sub>2</sub> nanorods is found to be much better than that of the commercial micro-sized. No studies of the effect on the photocatalytic efficiency of β-MnO<sub>2</sub> nanorods in the degradation of methylene blue, of parameters such as particle size, morphology and pyrolysis temperature were performed.

### Ir and Rh oxides

Metal oxides semiconductors arising from the so-called precious, among other, Ir, and Rh they are highly active in several catalysis processes. Of these, the iridium is most catalytically active [46]. Their activity is hugely enhanced at the nano-level [46, 49]. This metal, as well as their metal oxides, exhibits a high catalytic activity [46, 47]. Next, we will analyze a few results about the photocatalytic capacity of Ir and Rh oxides.

$\text{IrO}_2$  has an adequate bandgap of 2.4–2.6 eV [22] for the degradation of methylene blue under UV-visible irradiation.  $\text{IrO}_2$  prepared from a solid state thermal treatment of the PSP-4-PVP( $\text{IrCl}_3$ ) $_x$  precursor exhibits better photocatalytic activity (57% photodegradation in 300 min) than  $\text{IrO}_2$  prepared from Chitosan( $\text{IrCl}_3$ ) $_x$  precursor (38% photodegradation in 300 min). This effect was associated with the more porous morphology of  $\text{IrO}_2$  from the PSP-4-PVP ( $\text{IrCl}_3$ ) $_x$  precursor. In the literature there are no works on oxide  $\text{IrO}_2$  photocatalysis in the degradation of methylene blue or other dyes.

On the other hand, the bandgap values of  $\text{Rh}_2\text{O}_3$  3.7 eV is adequate for photocatalytic activity under UV-visible irradiation [23]. The results indicate that the sample exhibits photocatalytic activity 70% photodegradation in 300 min. Again, the high porosity of the materials can explain the relatively high photodegradation efficiency of the rhodium oxide. Here again the factor b, morphology, equation 1 could be the most important in to explain the relatively high photocatalytic efficiency toward the degradation of methylene blue pollutant. No studies of the effect on the photocatalytic efficiency of  $\text{Rh}_2\text{O}_3$  in the degradation of methylene blue, of parameters such as morphology, particle size, band gap and pyrolysis temperature were performed. No other photocatalytic degradation studies of methylene blue using  $\text{Rh}_2\text{O}_3$  have been found in literature, so no comparison was possible.

### ReO<sub>3</sub>

The bandgap for  $\text{ReO}_3$  4.36 eV, indicates an adequate value for UV-visible photoactivation [21]. Then  $\text{ReO}_3$  was also found to catalyze the photodegradation of MB with an efficiency of 53% and 64% in 300 min using a solid state method from thermal treatment of the Chitosan ( $\text{ReCl}_3$ ) and PSP-4-PVP( $\text{ReCl}_3$ ) $_n$  precursors, respectively. Despite this, their catalytic activity has only been proved in the catalytic degradation of methyl orange found a high photocatalytic efficiency [50]. No studies of the effect on the photocatalytic efficiency of  $\text{ReO}_3$  in the degradation of methylene blue, of parameters such as particle size, band gap and pyrolysis temperature or morphology were performed. Therefore, there is no data on the photocatalytic degradation of methylene blue with this oxide for its comparison.

### ThO<sub>2</sub>

Although  $\text{ThO}_2$  has a band gap of 5.66 eV and 5.75 eV [25] using Chitosan-( $\text{Th}(\text{NO}_3)_4$ ) $_n$  and d PS-4-co-PVP-( $\text{Th}(\text{NO}_3)_4$ ) $_n$  as precursor respectively, which would be close to an insulating behavior, an efficient capacity as a photocatalyst against methylene blue with values of 66% and 67% degradation in 300 min for  $\text{ThO}_2$ , obtained from Chitosan-( $\text{Th}(\text{NO}_3)_4$ ) $_n$  and from PS-4-co-PVP-( $\text{Th}(\text{NO}_3)_4$ ) $_n$  respectively, was observed [25]. SEM analyses have showed a high porous  $\text{ThO}_2$  for obtained from both Chitosan-( $\text{Th}(\text{NO}_3)_4$ ) $_n$  and PS-4-co-PVP-( $\text{Th}(\text{NO}_3)_4$ ) $_n$  as precursor. In such a way that the factor, b particle morphology, of equation 1, seems to be the predominant factor and cause of the photocatalytic activity of  $\text{ThO}_2$ . No studies of the effect on the photocatalytic efficiency of  $\text{ThO}_2$  in the degradation of methylene blue, of parameters such as particle size, band gap and pyrolysis temperature were performed. To our best knowledge no photodegradation studies of  $\text{ThO}_2$  towards organic dyes have appeared.

## GENERAL DISCUSSION

From the above discussion of suggests that in many cases the photocatalytic efficiency is dominated by the morphology of the photocatalyst material that is the factor b of equation 2.

Such is the case of  $\text{TiO}_2$ , where porous nanofibers achieve a high value in photocatalytic efficiency against methylene blue. Also for  $\text{CuO}$  prepared by Bharali, its photocatalytic efficiency against methylene blue degradation was attributed to the porosity of the photocatalyst prepared by this method. Also for  $\text{Fe}_2\text{O}_3$  prepared by Diaz et.al. The high efficiency in the photocatalytic degradation of methylene blue was attributed to a highly porous morphology. On the other hand,  $\text{Fe}_2\text{O}_3$  prepared by Lassoued, showed a good photocatalytic efficiency, which was attributed to a porous morphology of the sample used. For  $\text{SnO}_2$  prepared by Sadeghzadeh-Attar they show that the highest photocatalytic efficiency for the nanotubes of  $\text{SnO}_2$  photocatalyst was achieved by calcining the precursor at 600 °C. This can be attributed, among others, to the highly porous nature of nanotubes [41]. Therefore, in this study, the calcination temperature of

the  $\text{SnO}_2$  nanotubes played also an important role in the degradation of the MB dye. In many cases it occurs that the morphology depends on the calcination temperature of the photocatalyst. Then in equation 2 it must be considered that often, morphology = F (T calcination).

For  $\text{ThO}_2$  high porous nanomaterials for obtained from both Chitosan-( $\text{Th}(\text{NO}_3)_4$ ) $_n$  and PS-4-co-PVP-( $\text{Th}(\text{NO}_3)_4$ ) $_n$  as precursor was the main factor of its high photocatalytic capacity, factor, b particle morphology, of equation 2.

## CONCLUSIONS

1. There are very few studies on the photocatalytic degradation of polluting dyes using solid state photocatalyst.
2. From the few studies on photocatalytic degradation of polluting dyes such as methylene blue and using solid state photocatalyst, it can be concluded that in most cases the predominant factor in photocatalytic efficiency is porous morphology.
3. There are very few studies where the influence of other factors on photocatalytic efficiency is studied, such as particle size, band gap and temperature used in the heat treatment of the photocatalyst preparation.
4. In order to predictively use the multifactorial equation of the efficiency of a photocatalyst as a function of factors such as morphology, particle size, band gap, and pyrolysis temperature, it is necessary to investigate many photocatalytic studies in detail the influence of these factors on the photocatalytic efficiency.

Therefore, the need to develop catalysts in the solid state is a constant challenge [51-69]. In addition, the need for new studies of photocatalysis in the degradation of polluting organic dyes, contemplating effects of morphology, particle size, band gap and heating temperature in the preparation of the solid-state photocatalyst is an urgent need.

The realization of all these objectives could lead to the preparation of highly efficient photocatalyst, which would in turn to produce a significant leap in the environmental decontamination of liquid systems.

## REFERENCES

- 1.- Masciangoli, T.; Zhang, W. Environmental Technologies. *Environ. Sci. Technol.* **2003**, *37*, 102–108.
2. Vaseashta, A.; Vaclavikova, M.; Vaseashta, S.; Gallios, G.; Roy, P.; Pummakarnchana, O. Nanostructures in environmental pollution detection, monitoring, and remediation. *Sci. Technol. Adv. Mater.* **2007**, *8*, 47–59.
3. Khan, F.I.; Ghoshal, A.K. Removal of Volatile Organic Compounds from polluted air. *J. Loss Prev. Process Ind.* **2000**, *13*, 527–545.
4. Allahveran, S. Mehrzad, A., Polyaniline/ZnS nanocomposite as a novel photocatalyst for removal of Rhodamine 6G from aqueous media: optimization of influential parameters by response surface methodology and kinetic modeling. *J. Mol. Liq.* **2017**, *225*, 339–346.
- 5.-Rashi Gusain,R., Kanika Gupta K., Pratiksha Joshi P., Om P. Khatri P., Adsorptive removal and photocatalytic degradation of organic pollutants using metal oxides and their composites: *A comprehensive review*. Advances in Colloid and Interface Science **(2019)**, *272*, 102008.
- 6.- Chan S.,H.,S., WuT., Joon Ching Juanb,J.C.-,Teh.C.Y., Recent developments of metal oxide semiconductors as photocatalysts in advanced oxidation processes (AOPs) for treatment of dye waste-water, *J Chem Technol Biotechnol*, **2011**, *86*, 1130–1158
- 7.- Diaz,C., Valenzuela, M.L., Laguna-Bercero, M.A.Solid-State Preparation of Metal and Metal Oxides Nanostructures and Their Application in Environmental Remediation, *Int. J. Mol. Sci.* **2022**, *23*, 1093-1122.
- 8.- Khan M.K., Abdullah Al-Mayouf A., Adil S.F., Metal oxides as photocatalyst, *Journal of Saudi Chemical Society*, **2015** *19*, 462–46
- 9.- Warsia,M.F., N.S., Muhammad, Sarwarb I., Philips O. Agboolac P.O., Imran Shakird I., Sonia Zulfiqare, S. A, Comparative study on photocatalytic activities of various transition metal oxides nanoparticles synthesized by wet chemical route, *Desalination and Water Treatment*,**2021**,*211* 181–195.
- 10.- Diaz,C., Segovia,M., Valenzuela, M.L. Solid State Nanostructured Metal Oxides as Photocatalysts and Their Application in Pollutant Degradation: A Review, *Photochem.* **2022**, *2*, 609–627.
- 11.- Yadav S., Shakya K., Gupta A., Singh D., Chandran A.R., Aanappalli A.V., Kanika Goyal K., Rani N. Saini K. Review on degradation of organic dyes

- by using metal oxide semiconductors, *Environmental Science and Pollution Research*, **2023**, 30, 71912–71932
12. Kumari H., Suman S., Rohit Ranga R., Surjeet Chahal S., Seema Devi S., Sourabh Sharma S., Sandeep Kumar S., Kumar P., Suresh Kumar K., Ashok Kumar A., Rajesh Parmar R., Review on Photocatalysis Used For Wastewater Treatment: Dye Degradation, *Water Air Soil Pollut*, **2023**, 234, 349.
  - 13.- Tong, H.; Ouyang, S.; Bi, Y.; Umezawa, N.; Oshikiri, M.; Ye, J. Nano-photocatalytic materials: Possibilities and challenges. *Adv. Mater.* **2012**, 24, 229–251.
  14. Zhao, X.; Lv, L.; Pan, B.; Zhang, W.; Zhang, S.; Zhang, Q. Polymer-supported nanocomposites for environmental application: A review. *Chem. Eng. J.* **2011**, 170, 381–394.
  15. Mauter, M.; Elimelech, M. Environmental applications of carbon-based nanomaterials. *Environ. Sci. Technol.* **2008**, 42, 5843–5859.
  16. Sharma, Y.C.; Srivastava, V.; Singh, V.K.; Kaul, S.N.; Weng, C.H. Nano-adsorbents for the removal of metallic pollutants from water and wastewater. *Environ. Technol.* **2009**, 30, 583–609.
  17. Gui, X.; Wei, J.; Wang, K.; Cao, A.; Zhu, H.; Jia, Y.; Shu, Q.; Wu, D. Carbon nanotube sponges. *Adv. Mater.* **2010**, 22, 617–621.
  18. Ng, L.Y.; Mohammad, A.W.; Leo, C.P.; Hilal, N. Polymeric membranes incorporated with metal/metal oxide nanoparticles: A comprehensive review. *Desalination* **2013**, 308, 15–33.
  - 19.- Khan I., Saeed K., Zekker I., Zhang B., Hendi A.H., Ahmad A., Ahmad S., Zada N., Ahmad H., Luqman Ali Shah L.A., Shah T., Khan I., Review on Methylene Blue: Its Properties, Uses, Toxicity and Photodegradation, *Water* **2022**, 14, 242.
  - 20.-Allende P, Laguna M.A, Barrientos L, Valenzuela M.L, Diaz C. Solid State Tuning Morphology, Crystal Phase and Size through Metal Macromolecular Complexes and Its Significance in the Photocatalytic Response, *ACS Applied Energy and Materials* **2018**, 1, 3159-3170.
  - 21.- Diaz C, Valenzuela M.L, Cifuentes-Vaca O, Segovia M, Laguna-Bercero M.A. Incorporation of Nanostructured ReO<sub>3</sub> in Silica Matrix and Their Activity Toward Photodegradation of Blue Methylene. *Journal of Inorganic and Organometallic Polymers and Materials* **2020**, 30, 1726–1734.
  22. Diaz C, Valenzuela M.L, Cifuentes-Vaca O, Segovia M, Laguna-Bercero M.A. Iridium nanostructured metal oxide, its inclusion in Silica matrix and their activity toward Photodegradation of Methylene Blue. *Materials Chemistry and Physics* **2020**, 252, 123276-123286
  23. Diaz C, Valenzuela M.L, Cifuentes-Vaca O, Segovia M. Polymer precursors effect in the macromolecular metal-polymer on the Rh/RhO<sub>2</sub>/Rh<sub>2</sub>O<sub>3</sub> phase using solvent-less synthesis and its photocatalytic activity. *Journal of Inorganic and Organometallic Polymers and Materials* **2020**, 30, 4702-4708.
  - 24.- Diaz C, Valenzuela M.L, Cifuentes-Vaca O, Segovia M, Laguna-Bercero M.A. Incorporation of NiO into SiO<sub>2</sub>, TiO<sub>2</sub>, Al<sub>2</sub>O<sub>3</sub>, and Na<sub>4.2</sub>Ca<sub>2.8</sub>(Si<sub>6</sub>O<sub>18</sub>) Matrices, Medium Effect on the Optical Properties and Catalytic Degradation of Methylene Blue, *Nanomaterials* **2020**, 10, 2470-2487.
  25. Diaz C, Valenzuela M.L, Laguna-Bercero M.A, Mendoza K, Cartes P. Solventless preparation of thorium, their inclusion inside SiO<sub>2</sub> and TiO<sub>2</sub>, their luminescent properties and their photocatalytic behavior. *ACS Omega* **2021**, 6, 14, 9391–9400.
  - 26.- Gaya,U.I, Abdullah A.H., Heterogeneous photocatalytic degradation of organic contaminants over titanium dioxide: A review of fundamentals, progress and problems *J. Photochem. Photobiol. C* **2008**, 9, 1-12.
  - 27.- Joshi N.C.,Gururani P., Gairola S.P, Metal Oxide Nanoparticles and their Nanocompositebased Materials as Photocatalysts in the Degradation of Dyes,*Biointerface Research in Applied Chemistry* **2022**,12, 6557-6579.
  - 28.- Kusuma K.B. , Manju M.\* , Ravikumar C.R. , Raghavendra N. , Amulya S., Nagaswarupa H.P., Ananda Murthy H.C., M.R. Kumar A., Shashi Shekhar T.R. , Photocatalytic degradation of Methylene Blue and electrochemical sensing of paracetamol using Cerium oxide nanoparticles synthesized via sonochemical route, *Applied Surface Science Advances* **2022**, 11,100304.
  - 29.- Pouretedal H.R. \*, Kadhodaie A., Synthetic CeO<sub>2</sub> Nanoparticle Catalysis of Methylene Blue Photodegradation: Kinetics and Mechanism, *Chin. J. Catal*, **2010**, 31, 1328–1334.
  - 30.- Saravanan R., Gupta V.K., Narayanan V. , Stephen A., Comparative study on photocatalytic activity of ZnO prepared by different methods, *Journal of Molecular Liquids* **2013**, 181, 133–141.
  - 31.- Riapanitra A., Riyani K., Setyaningtyas T., Photocatalytic and Kinetics Study of Copper Oxide on the Degradation of Methylene Blue Dye, *Advances in Physics Research*, **2022**, 5, 1-5.
  - 32.- Deka P., Deka R.C., Bharali P., Porous CuO nanostructure as a reusable catalyst for oxidative degradation of organic water pollutants ,*New J. Chem.*, **2016**, 40, 348—357.
  - 33.-Meshram S.P., Adhyapak P.V., Mulik U.P., Amalnerkar D.P. , Facile synthesis of CuO nanomorphs and their morphology dependent sunlight driven photocatalytic properties , *Chemical Engineering Journal*,**2012**, 204–206, 158–168.
  - 34.- Diaz, C.; Valenzuela, M.L.; Cifuentes-Vaca, O.; Segovia, M.; Laguna-Bercero, M.A. Incorporation of NiO into SiO<sub>2</sub>, TiO<sub>2</sub>, Al<sub>2</sub>O<sub>3</sub>, and Na<sub>4.2</sub>Ca<sub>2.8</sub>(Si<sub>6</sub>O<sub>18</sub>) Matrices, Medium Effect on the Optical Properties and Catalytic Degradation of Methylene Blue. *Nanomaterials* **2020**, 10, 2470.
  - 35.-Khairnar S.D., Shrivastava V., Facile synthesis of nickel oxide nanoparticles for the degradation of Methylene blue and Rhodamine B dye: a comparative study, *Journal of Taibah University for Science*, **2019**, 13:1, 1108-1118.
  - 36.- Diaz, C.; Barrera, G.; Segovia, M.; Valenzuela, M.L.; Osiak, M.; O'Dwyer, C. Solvent-less method for efficient photocatalytic  $\alpha$ -Fe<sub>2</sub>O<sub>3</sub> nanoparticles for using macromolecular polymeric precursors". *New J. Chem.* **2016**, 40, 6768-6776.
  - 37.-Khalaji A.D., Spherical  $\alpha$ -Fe<sub>2</sub>O<sub>3</sub> Nanoparticles: Synthesis and Characterization and Its Photocatalytic Degradation of Methyl Orange and Methylene Blue, Spherical  $\alpha$ -Fe<sub>2</sub>O<sub>3</sub> Nanoparticles: Synthesis and Characterization and Its Photocatalytic Degradation of Methyl Orange and Methylene Blue, *Phys. Chem. Res.*, **2022**, 10, 473-483.
  - 38.- Lassoued A., Mohamed Saber Lassoued M.S., Brahim Dkhal B., Ammar S.,Abdellatif Gadri,S., Photocatalytic degradation of methylene blue dye by iron oxide ( $\alpha$ -Fe<sub>2</sub>O<sub>3</sub>) nanoparticles under visible irradiation, *Journal of Materials Science: Materials in Electronics* .**2018**, 29,8142–8152.
  - 39.- Liu J., Wang B., Li Z., Wu Z., Kongjun Zhu, Zhuang J., Xi Q., Hou Y., Jiankang Chen J., Cong M., Li J., Qian G., Lin, Z., Photo-Fenton reaction and H<sub>2</sub>O<sub>2</sub> enhanced photocatalytic activity of  $\alpha$ -Fe<sub>2</sub>O<sub>3</sub> nanoparticles obtained by a simple decomposition route, *Journal of Alloys and Compounds* **2019** 771,398-405.
  - 40.- Quinteros E., Eder Lugo Medina E.L., Quevedo R.V., Garrafa H.E., Baez Y.A., Vargas F.A., Rafael Vilchis A.R, Luque P.A., A Study of the Optical and Structural Properties of SnO<sub>2</sub> Nanoparticles Synthesized with Tilia cordata Applied in Methylene Blue Degradation, *Symmetry* **2022**, 14, 2231.
  - 41.- Sadeghzadeh-Attar A., Efficient photocatalytic degradation of methylene blue dye by SnO<sub>2</sub> nanotubes synthesized at different calcination temperatures, *Solar Energy Materials and Solar Cells* **2018**,183, 16–24,
  - 42.-Kima S.P., Choib M.Y., Choia H.C., Photocatalytic activity of SnO<sub>2</sub> nanoparticles in methylene blue degradation, *Materials Research Bulletin* **2016**,74, 85–89
  - 43.- Warang T., Patel N., Fernandes R., Bazzanella N., MiotelloA., Co<sub>3</sub>O<sub>4</sub> nanoparticles assembled coatings synthesized by different techniques for photo-degradation of methylene blue dye, *Applied Catalysis B: Environmental* **2013**, 132–133 204–211.
  - 44.- Bazgir S., Farhadi S., Microwave-assisted rapid synthesis of Co<sub>3</sub>O<sub>4</sub> nanorods from CoC<sub>2</sub>O<sub>4</sub> .2H<sub>2</sub> O nanorods and its application in photocatalytic degradation of methylene blue under visible light irradiation, *Int. J. Nano Dimens.* **2017**, 8, 284-297.
  - 45.- Zhang W., Yang Z., Wang X., Zhang Y., Wen X., Shihe Yang b, Large-scale synthesis of b-MnO<sub>2</sub> nanorods and their rapid and efficient catalytic oxidation of methylene blue dye, *Catalysis Communications* **2006**, 7, 408-412.
  - 46.- Cotton, F.A.; Wilkinson, G. *Advanced Inorganic Chemistry*; John Wiley and Sons: New York, NY, USA, 1980; Chapters 22 and 30. 64.
  - 47.- Jin, R. The impacts of nanotechnology on catalysis by precious metal nanoparticles. *Nanotechnol. Rev.* **2012**, 31–56.
  - 48.- Fernandez-Garcia, M.; Martinez-Arias, A.; Hanson, J.; Rodriguez, C. Nanostructured Oxides in Chemistry: Characterization and Properties. *Chem. Rev.* **2004**, 104, 4063–4104.
  - 49.- Zhao, Y.; Hernandez, E.A.; Vargas-Barbosa, N.M.; Dysart, J.L.; Mallouk, T.E. A high yield Synthesis of ligand-free iridium oxide nanoparticles with high electrocatalytic activity. *J. Phys. Chem. Lett.* **2011**, 2, 402–406.
  - 50.- Biswas, K.; Rao, C.N. Synthesis and Characterization of Nanocrystals of the Oxide Metals, RuO<sub>2</sub>, IrO<sub>2</sub>, and ReO<sub>3</sub>. *J. Nanosci. Nanotechnol* **2007**, 7, 1969–1974.

- 51.-Díaz, C.; Valenzuela, M.L. Metallic Nanostructures Using Oligo and Polyphosphazenes as Template or Stabilizer in Solid State. In Encyclopedia of Nanoscience and Nanotechnology; Nalwa, H.S., Ed.; American Scientific Publishers: Valencia, CA, USA, 2010; Volume 16, pp. 239–256.
- 52.- Díaz, C.; Valenzuela, M.L. Macromolecular Complexes MX<sub>n</sub> Polymer as solid state precursors of metal and metal oxides nanostructures. In Book of CRC Concise Encyclopedia of Nanotechnology; Kharisov, B.I., Kharisov, O.V., Mendez, U., Eds.; CRC Press: Boca Raton, FL, USA, 2016; Chapter 42; pp. 504–524.
- 53.- Díaz, C.; Valenzuela, M.L. Small-Molecule and High-Polymeric Phosphazenes containing oxypyridine side groups and their organometallic derivatives; Useful precursors for metal nanostructured materials. *Macromolecules* **2006**, 39, 103–111.
54. Díaz, C.; Valenzuela, M.L. Organometallic Derivatives of Polyphosphazenes as Precursors for Metallic Nanostructured Materials. *J. Inorg. Organomet. Polym. Mater.* **2006**, 16, 419–435.
55. Díaz, C.; Valenzuela, M.L.; Zuñiga, L.; O'Dwyer, C. Organometallic derivatives of cyclotriphosphazene as precursors of Nanostructured metallic materials: A new solid state Method. *J. Inorg. Organomet. Polym. Mater.* **2009**, 19, 507–520
56. Díaz, C.; Valenzuela, M.L.; Lavayen, V.; O'Dwyer, C. Layered Graphitic Carbon Host Formation during Liquid-free Solid State Growth of Metal Pyrophosphates. *Inorganic Chem.* **2012**, 51, 6228–6236.
57. Díaz, C.; Valenzuela, M.L.; Cáceres, S.; O'Dwyer, C. Solution and surfactant-free growth of supported high index facet SERS active nanoparticles of rhenium by phase demixing. *J. Mater. Chem. A* **2013**, 1, 1566–1572.
- 58.- Díaz, C.; Valenzuela, M.L.; Cáceres, S.; O'Dwyer, C.; Diaz, R. Solvent and stabilizer free growth of Ag and Pd nanoparticles using Metallic salts/cyclotriphosphazenes mixtures. *Mater. Chem. Phys.* **2013**, 143, 124–132.
59. Díaz, C.; Valenzuela, M.L.; Zuñiga, L.; O'Dwyer, C. Solid State Pathways to Complex Shape Evolution and Tunable Porosity During Metallic Crystal Growth. *Sci. Rep.* **2013**, 2642, 1–8.
60. Díaz, C.; Valenzuela, M.L. Nanostructures: Properties: Production Methods and Application. In Organometallic-Metallic Cyclotriphosphazene Mixtures: Solid-State Method for Metallic Nanoparticle Growth; Nova Science Publishers: New York, NY, USA, 2013; Chapter 5.
61. Díaz, C.; Valenzuela, M.L. A General Solid-State Approach to Metallic, Metal Oxides and Phosphates Nanoparticles in Advances in Chemical Research; Nova Science Publishers: New York, NY, USA, 2011.
62. Díaz, C.; Valenzuela, M.L. A general Solid-State approach to Metallic, Metal oxides and Phosphate nanoparticles Gold Nanoparticles: Properties Synthesis and Fabrication. In Solution and Solid State Methods to Prepare Au Nanoparticles: A comparison Chow PE; Nova Science Publishers: New York, NY, USA, 2010; Chapter 14.
63. Díaz, C.; Valenzuela, M.L.; Lavayen, V.; Mendoza, K.; Peña, O.; O'Dwyer, C. Nanostructured copper oxides and phosphates from a new solid-state route. *Inorg. Chim. Acta* **2011**, 377, 5–11.
64. Díaz, C.; Platoni, S.; Molina, A.; Valenzuela, M.L.; Geaney, H.; O'Dwyer, C. Novel Solid-State Route to Nanostructured Tin, Zinc and Cerium Oxides as Potential Materials for Sensors. *J. Nanosci. Nanotechnol* **2014**, 14, 7648–7675.
65. Díaz, C.; Valenzuela, M.L.; Laguna, M.A.; Orera, A.; Bobadilla, D.; Abarca, S.; Peña, O. Synthesis and Magnetic Properties of Nanostructured metallic Co, Mn and Ni oxide materials obtained from solid-state macromolecular complex precursors. *RSC Adv.* **2017**, 7, 27729–27736.
66. Díaz, C.; Valenzuela, M.L.; Bobadilla, D.; Laguna-Bercero, M.A. Bimetallic Au//Ag Alloys Inside SiO<sub>2</sub> using a solid-state method. *J. Clust. Chem.* **2017**, 28, 2809–2815.
67. Díaz, C.; Valenzuela, M.L.; Garcia, C.; De la Campa, R.; Soto, A.-P. Solid-state synthesis of pure and doped lanthanides oxide nanomaterials by using polymer templates. Study of their luminescent properties. *Mater. Lett.* **2017**, 209, 111–114.
68. Díaz, C.; Valenzuela, M.L.; Segovia, M.; De la Campa, R.; Soto, A.-P. Solution, Solid-State Two Step Synthesis and Optical Properties of ZnO and SnO<sub>2</sub> Nanoparticles and Their Nanocomposites with SiO<sub>2</sub>. *J. Clust. Sci.* **2018**, 29, 251–266.
69. Díaz, C.; Carrillo, D.; De la Campa, R.; Soto, A.-P.; Valenzuela, M.L. Solid-State synthesis of LnOCl/Ln<sub>2</sub>O<sub>3</sub> (Ln = Eu, Nd) by using chitosan and PS-co-P4VP as polymeric supports. *J. Rare Earth* **2018**, 36, 1326–1332.